International Journal of Science and Research (IJSR)
ISSN (Online): 2319-7064
Index Copernicus Value (2015): 78.96 | Impact Factor (2015): 6.391

Unsteady MHD Flow of non-Newtonian Fluid through Past Vertical Stretching Sheet

Dr. P. Sulochana

Department of Mathematics, Intell Engineering College, Anantapuramu.

Abstract: ***In this paper, we have considered the MHD flow of an electrically conducting non-Newtonian fluid past a vertical stretching sheet. Convective boundary conditions, thermophoresis and thermal radiation are taken into account. The governing equations reduced into a dimensionless form making use of similarity transformations. The confined similarity equations are originated and solved using shooting method together with Runge–Kutta sixth order system. The flow characteristics are discussed through graphs and tables. The investigation walk around that, the fluid velocity and temperature in the boundary layer region get higher significantly for increasing the values of thermal radiation parameter. The Nusselt number enhances with increasing the values of the surface convection parameter.***

Keywords: Convective boundary conditions; MHD flows; porous medium; stretching sheets

1. Introduction

Non-Newtonian fluid flows generated by a stretching sheet have been widely analyzed for the importance in several manufacturing processes such as extrusion of molten polymers through a slit die for the production of plastic sheets, processing of food stuffs, paper production, and wire and fiber coating. On the other hand, convective heat transfer plays a vital role during the handling and processing of non-Newtonian fluid flows. Mechanics of non-Newtonian fluid flows present a special challenge to engineers, physicists, and mathematicians. Because of the complexity of these fluids, there is not a single constitutive equation which exhibits all properties of such non Newtonian fluids. In the process, a number of nonNewtonian fluid models have been proposed. The vast majority of non-Newtonian fluid are concerned of the types, e.g., like the power-law and grade two or three (Serdar and Salih Dokuz (2006), Andersson and Dandapat (1992), Sadeghy and Sharifi (2004), Hassanien (1996), Sajid et al. (2007, 2009), Keimanesha et al. (2011), Rashidi et al. (2012)). These simple fluid models have the shortcomings that render results that are not in accordance with the fluid flows in reality. Power-law fluids are by far the most widely used model to express nonNewtonian behavior in fluids. The model predicts shear thinning and shear thickening behavior. However, it is inadequate in expressing normal stress behavior as observed in die swelling and rod climbing behavior in some non-Newtonian fluids. In order to obtain a thorough cognition of nonNewtonian fluids and their various applications, it is necessary to study their flow behaviors. Due to their application in industry and technology, few problems in fluid mechanics have enjoyed the attention that has been accorded to the flow which involves non-Newtonian fluids. The non-linearity can manifest itself in a variety of ways in many fields, such as food, drilling operations and bioengineering. The Navier–Stokes theory is inadequate for such fluids, and no single constitutive equation is available in the literature which exhibits the properties of all fluids. Because of the complexity of these fluids, there is not a single constitutive equation which exhibits all properties of such non-Newtonian fluids. Thus, a number of non-Newtonian fluid models have been proposed. The Casson model is a well-known rheological model for describing the nonNewtonian flow behavior of fluids with a yield stress as Casson (1959). The model was developed for viscous suspensions of cylindrical particles by Reher et al. (1969). Regardless of the form or type of suspension, some fluids are particularly well described by this model because of their nonlinear yield-stress-pseudoplastic nature. Examples are blood as Cokelet et al. (1963), chocolate by Chevalley (1991), xanthan gum solutions by Garcia-Ochoa and Casas (1994). The Casson model fits the flow data better than the more general Herschel–Bulkley model by Joye (1998) and Kirsanov, and Remizo (1999), which is a power-law formulation with yield stress as Bird et al. (1960). For chocolate and blood, the Casson model is the preferred rheological model. It seems increasingly that the Casson model fits the nonlinear behavior of yield-stress-pseudoplastic fluids rather well and it has therefore gained in popularity since its introduction in 1959. It is relatively simple to use, and it is closely related to the Bingham model Bird et al. (1960), which is very widely used to describe the flow of slurries, suspensions, sludge, and other rheologically complex fluids as Churchill (1988). Eldabe and Salwa (1995) have studied the Casson fluid for the flow between two rotating cylinders, and Boyd et al. (2007) investigated the Casson fluid flow for the steady and oscillatory blood flow. Boundary layer flow of Casson fluid over different geometries is considered by many authors in recent years. Nadeem et al. (2012) presented MHD flow of a Casson fluid over an exponentially shrinking sheet. Kumari et al. (2011) analyzed peristaltic pumping of a MHD Casson fluid in an inclined channel. Sreenadh et al. (2011) studied the flow of a Casson fluid through an inclined tube of non uniform cross-section with multiple stenoses. Mernone and Mazumdar (2002) discussed the peristaltic transport of a Casson fluid. Porwal and Badshah (2012) work on steady blood flow with Casson fluid along an inclined plane influenced by the gravity force. Mukhopadhyay et. al. (2013) studied the unsteady two-dimensional flow of a non-Newtonian fluid over a stretching surface having a prescribed surface temperature, the Casson fluid model is used to characterize the nonNewtonian fluid behavior. Abolbashari et al. (2015) have been reported an analytical investigation of the fluid flow, heat and mass transfer and entropy generation for the

steady laminar non-Newtonian nano-fluid flow induced by a stretching sheet in the presence of velocity slip and convective surface boundary conditions using optimal homotopy analysis method (HAM). Suction or blowing process has also have their importance in many engineering activities, for example, in the design of thrust bearing and radial diffusers, and thermal oil recovery. Suction is applied to chemical processes to remove reactants. Blowing is used to add reactants, which cool the surface, prevent corrosion or scaling and reduce the drag. In mass transfer cooling, can significantly change the flow field and, as a consequence, affects the heat transfer rate from the plate (see Shridan et al. (2006), Chamkha et al. (2010), Yih (1998), Tsai et al. (2008), Ishak et al. (2009)). In addition, a combined free and forced convection flow of an electrically conducting fluid in the presence of a transverse magnetic field is of special technical significance because of its frequent occurrence in many industrial applications such as geothermal reservoirs, cooling of nuclear reactors, thermal insulation, petroleum reservoirs, etc. This type of problem also arises in electronic packages, microelectronic devices during their operations. In recent years, several convection heat transfer and fluid flow problems have received new attention within the more general context of MHD.

In this present paper, the heat and mass transfer on MHD flow of an electrically conducting non-Newtonian fluid over a semi-infinite vertical stretching sheet.

2. Formulation and Solution of the Problem

Consider the steady boundary layer flow of an incompressible and electrically conducting non-Newtonian (Visco-elastic) fluid past a stretching sheet coinciding with the plane $y=0$ and the flow being confined to $y>0$ in the presence of viscous dissipation and joule heating. The flow is generated, due to the stretching of the sheet caused by the simultaneous action of two equal and opposite forces along the x-axis. The sheet is then stretched with a velocity $u_w(x)=ax$, where a is a constant and x is the coordinate measured along the stretching surface from the slit. The thermal radiation is taking place in the flow and the effect of thermophoresis is being taken into account to help in understanding of the mass deposition variation on the surface. A uniform transverse magnetic field of strength B_0 is applied parallel to the y-axis. The applied magnetic field and magnetic Reynolds number are assumed to be very small so that the induced magnetic field and the Hall effect are negligible. It is assumed that there is no applied voltage which implies the absence of an electric field. The stretching surface is maintained at constant temperature T_w higher than the constant temperature T_∞ of the ambient fluid. Due to the boundary layer behavior the temperature gradient along y-direction is much more than that along x-direction and hence only the thermophoretic velocity component which is normal to the surface is of importance. Under these assumptions, the governing boundary layer equations for a non-Newtonian fluid flow can be written as [18, 36]

$$\frac{\partial u}{\partial x}+\frac{\partial v}{\partial y}=0 \tag{1}$$

$$u\frac{\partial u}{\partial x}+v\frac{\partial v}{\partial y}=\nu\frac{\partial^2 u}{\partial y^2}+\frac{\alpha_1}{\rho}\left[\frac{\partial}{\partial x}\left(u\frac{\partial^2 u}{\partial y^2}\right)-\frac{\partial u}{\partial y}\frac{\partial^2 u}{\partial x\partial y}+\nu\frac{\partial^3 u}{\partial y^3}\right]-\frac{\sigma B_0^2}{\rho}u+g\beta\left(T-T_\infty\right)+g\beta^*\left(C-C_\infty\right) \tag{2}$$

$$\rho c_p\left(u\frac{\partial T}{\partial x}+v\frac{\partial T}{\partial y}\right)=K\frac{\partial^2 T}{\partial y^2}-\frac{\partial q_r}{\partial y}+\mu\left(\frac{\partial u}{\partial y}\right)^2+\alpha_1\frac{\partial u}{\partial y}\left[\frac{\partial}{\partial y}\left(u\frac{\partial u}{\partial x}+v\frac{\partial u}{\partial y}\right)\right]+\left(\sigma B_0^2\right)u^2 \tag{3}$$

$$u\frac{\partial C}{\partial x}+v\frac{\partial C}{\partial y}=D_m\frac{\partial^2 C}{\partial y^2}+\frac{D_m K_T}{T_m}\frac{\partial^2 T}{\partial y^2}-\frac{\partial\left(V_T C\right)}{\partial y}-K_r\left(C-C_\infty\right) \tag{4}$$

Where all the physical quantities are of their usual meaning. $V_T=-\frac{K_1\nu}{T_r}\frac{\partial T}{\partial y}$ the thermophoretic velocity, We assume the bottom surface of the plate is heated by convection from a hot fluid at temperature T_w which provides a heat transfer coefficient h_w. The boundary conditions of the present model are

$$u=u_w, v=v_0, -k\frac{\partial T}{\partial y}=h_w\left(T_w-T\right), C=C_w \quad \text{at} \quad y=0 \tag{5}$$

$$u\to 0, \frac{\partial u}{\partial x}\to 0, T\to T_\infty, C\to C_\infty \quad \text{at} \quad y\to\infty \tag{6}$$

Where, v_0 is the suction/injection velocity.

Using the Rosseland approximation, the radiative heat flux term is given by [34]

$$q_r=-\frac{4\sigma^*}{3k^*}\frac{\partial T^4}{\partial y} \tag{7}$$

Assuming that the differences in the temperature within the flow are such that T^4 can be expressed as a linear combination of the temperature, we expand T^4 in Taylor's series about T_∞ and neglecting higher order terms, we get

$$T^4=4T_\infty^4 T-3T_\infty^4 \tag{8}$$

Thus we have

$$\frac{\partial q_r}{\partial y} = -\frac{16T_\infty^3\sigma^*}{3k^*}\frac{\partial^2 T}{\partial y^2} \quad (9)$$

Where, σ^* is the Stefan–Boltzmann constant and k^* is the mean absorption coefficient. the similarity transformations as given below are introduced:

$$\eta = \left(\frac{c}{\nu}\right)^{1/2} y,\ u = cxf'(\eta), v = -(c\nu)^{1/2} f(\eta), \theta(\eta) = \frac{T-T_\infty}{T_w - T_\infty}, \phi(\eta) = \frac{C-C_\infty}{C_w - C_\infty} \quad (10)$$

Eq. (1) is automatically satisfied. Using Eq. (9) in (3) and applying transformation (10), Eqs. (2) – (4) reduce to the ordinary differential equations:

$$f'^2 - ff'' - f''' - \lambda_1\left(2f'''f' - ff^{iv} - f''^2\right) + M^2 + f' - Gr\theta - Gm\phi = 0 \quad (11)$$

$$(1+Nr)\theta'' + \Pr f\theta' + \Pr Ec\left[f''^2 + M^2 f'^2 + \lambda_1 f''\left(f'f'' - ff'''\right)\right] = 0 \quad (12)$$

$$\phi'' + Sc\left(f - \tau\theta'\right)\phi' + Sc\left(Sr - \tau\phi\right)\theta'' - ScKr\phi = 0 \quad (13)$$

The boundary conditions (5, 6) then turn into

$$f = f_w, f' = 1, \theta' = -\gamma(1-\theta), \phi = 1 \quad \text{at} \quad \eta = 0 \quad (14)$$

$$f' \to 0, f'' \to 0, \theta \to 0, \phi \to 0 \quad \text{at} \quad \eta \to \infty \quad (15)$$

Here prime denotes differentiation with respect to η, where,

$\lambda_1 = \frac{\alpha_1 a}{\rho\nu}$ is the second grade fluid parameter, $M^2 = \frac{\sigma B_0^2}{\rho a}$ is the magnetic field parameter, $f_w = \frac{v_0}{(a\nu)^{1/2}}$ is the suction parameter, $Nr = \frac{16T_\infty^3\sigma^*}{3k^*K}$ is the thermal radiation parameter, $\Pr = \frac{\mu C_p}{K}$ is the Prandtl number, $Ec = \frac{u_w^2}{C_p(T_w - T_p)}$ is the Eckert number, $\tau = -\frac{k(T_w - T_p)}{T_r}$ is the thermophoretic parameter, $Sc = \frac{\nu}{D_m}$ is the Schmidt number, $Sr = \frac{D_m K_T (T_w - T_\infty)}{T_m \nu (C_w - C_\infty)}$ is the Soret number, $Gr = \frac{g\beta(T_w - T_\infty)}{a}$ is the thermal Grashof number, $Gm = \frac{g\beta^*(C_w - C_\infty)}{a}$ is the solutal Grashof number, $Kr = \frac{k_r \nu}{aD_m}$ is the chemical reaction parameter and $\gamma = \frac{h_w}{K(\nu/a)^{1/2}}$ is the surface convection parameter.

The physical quantities of practical and engineering primary interest are the skin friction coefficient, Nusselt number and Sherwood number. The equation defining the wall shear stress is

$$\tau_w = \left[\mu\frac{\partial u}{\partial y} + \rho\alpha_1\left(2\frac{\partial u}{\partial x}\frac{\partial u}{\partial y} + u\frac{\partial^2 u}{\partial x \partial y}\right)\right]_{y=0} \quad (15)$$

The local dimensionless skin friction coefficient is given by

$$C_f = 2\,\mathrm{Re}^{-1/2}\left[1 + 3\lambda_1 f'(0)\right]f''(0) \quad (16)$$

Or

$$C_f^* = \left[1 + 3\lambda_1 f'(0)\right]f''(0) \quad (17)$$

Where, $C_f^* = \frac{1}{2}\mathrm{Re}^{1/2} C_f$

Knowing the temperature field, it is interesting to study the effect of the free convection and thermal radiation on the rate of heat transfer q_w, is given by

$$q_w = -K\left(\frac{\partial T}{\partial y}\right)_{y=0} - \frac{16T_\infty^3\sigma^*}{3k^*}\left(\frac{\partial^2 T}{\partial y^2}\right)_{y=0} \quad (18)$$

So the rate of heat transfer in terms of dimensionless Nusselt number (*Nu*) is defined as follows:

$$Nu = -\mathrm{Re}^{1/2}(1+Nr)\theta'(0) \quad (19)$$

Or

$$Nu^* = -(1+Nr)\theta'(0) \quad (20)$$

Where, $Nu^* = \mathrm{Re}^{-1/2} Nu$

The rate of mass transfer in terms of dimensionless Sherwood number (*Sh*) is given by

$$Sh = -\mathrm{Re}^{1/2}\phi'(0) \quad (21)$$

Or

$$Sh^* = -\phi'(0) \quad (22)$$

Where, $Sh^* = \mathrm{Re}^{-1/2} Sh$

3. Results and Discussion

The numerical computations are performed using the method described in the previous section for various values of parameters that describe the flow characteristics of a second grade fluid over a convectively heated stretching

sheet. The set of Eqs. (11)–(13) under the boundary conditions (14) – (15) are solved numerically by applying the Shooting iteration technique together with Runge- Kutta sixth-order integration scheme. The following algorithm is used to solve the non-linear ordinary differential Eqs. (11)–(13) along with the boundary conditions (14): Reduce Eqs. (11)–(13) to a system of first order equations. Set the boundary conditions and initial values. Shooting technique to guess initial values. Repeat the step 3 until far filled boundary conditions are satisfied. Solve the reduced system of first order equations by Runge-Kutta method. Repeat these steps until the convergence criterion of 10^{-6} holds good.

The results are illustrated graphically in Figs. (2–4) and in Table 2. There are many parameters involved in the final form of the model. The problem can be protracted on many directions, but the first one seems to consider the effects of surface convection parameter, radiation parameter, second grade parameter and thermophoretic parameter. The default values of material parameters are considered in the simulation as M=2, Sr=0.5, Sc=0.64, λ1=1.5, Kr=0.2, γ=0.1, Gr=5, Gm=5, Pr=0.71, Nr=0.4, Ec=0.02 and τ=0.2 unless otherwise specified.

Figs. 1 displayed the behaviour of the velocity distribution for various values of thermal radiation parameter Nr. Fig. 1 shows that an increase in radiation parameter tends to increase the fluid velocity in the boundary layer region. The physics behind the results is that the thermal radiation increases the thickness of momentum boundary layer, which ultimately enhances the velocity. The effect of second grade parameter λ_1 on the fluid velocity distribution is illustrated in Figs. 2. The velocity component across the boundary layer reduces with an increase in the second grade parameter and also decreases asymptotically to zero at the edge of the hydro dynamic boundary layer. The effect of surface convection parameter γ on the stream wise velocity component is shown in Fig. 2. As the value of γ increases, the flow rate enhances and thereby giving rise to an increase in the velocity profiles as depicted in Fig. 3. Figs. 4 illustrate the variation of the velocity distribution for various values of thermophoretic parameter τ. The fluid velocity decreases with increase in the thermophoretic parameter and so the momentum boundary layer thickness decreases. The fluid velocity reduces with increasing the intensity of the magnetic field M or Pr or Sc. Increase the chemical reaction parameter Kr diminishes the velocity profile as shown the same figure. Likewise the magnitude of the velocity enhances with increasing Gr or Gm.

From Fig. 5, it is also observed that the temperature distribution increases uniformly with increasing thermal radiation parameter Nr. Thus, by escalating Nr, thermal boundary layer thickness enhances. The impact of surface convection parameter γ on fluid temperature in presence of thermal radiation is demonstrated in Fig. 6. It is observed from the figure that the fluid temperature increases with increase in γ in the boundary layer region. It is observed that with increase in the second grade parameter or second grade fluid parameter λ_1 (Figure 7), the temperature profiles increase and hence thickness of thermal boundary layer increases. From the figure (8), the temperature reduce reduces with increase in Pr, and hence thickness of thermal boundary layer decreases.

The concentration of the fluid decreases with increasing the values of Sc, Kr and thermophoretic parameter τ, and increases with Sr as presented in Fig. (9-12).

It is found from Table 2 that an increase in τ leads to an increase in both the values of the wall shear stress (in magnitude), Nusselt number and Sherwood number. It is observed that with increasing the values of λ_1, the reduced skinfriction coefficient (in absolute sense), Nusselt number diminishes whereas the Sherwood number increases. It can be seen from Table2 that the magnitude of the reduced skin friction coefficient decreases with increase in the radiation parameter Nr where as the thermal radiation increases the rate of heat transfer. It is observed that the heat transfer rate at the plate increases with increasing the values of γ whereas the effect is opposite for the wall shear stress (in magnitude) at the plate i.e. the reduced skin friction coefficient (in magnitude) decreases with increasing the surface convection parameter. The skin friction coefficient reduces with Kr and enhances with increasing M.

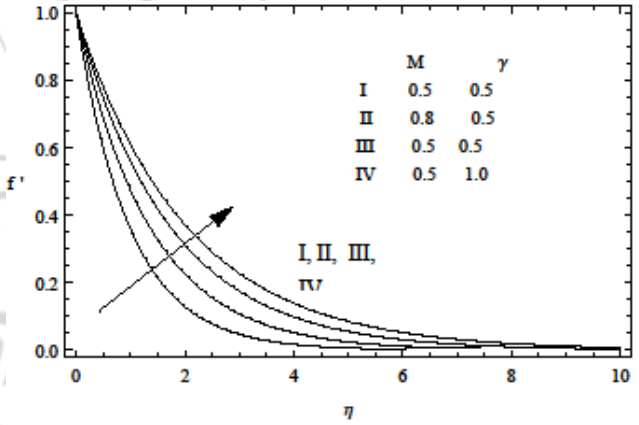

Figure 1: Velocity Profiles against M and γ

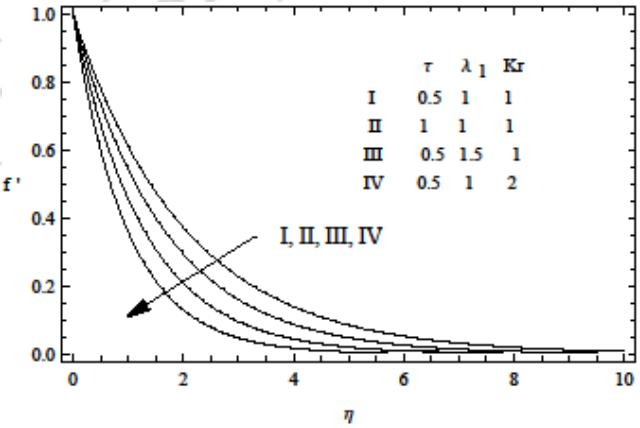

Figure 2: Velocity Profiles against τ , λ1, Kr

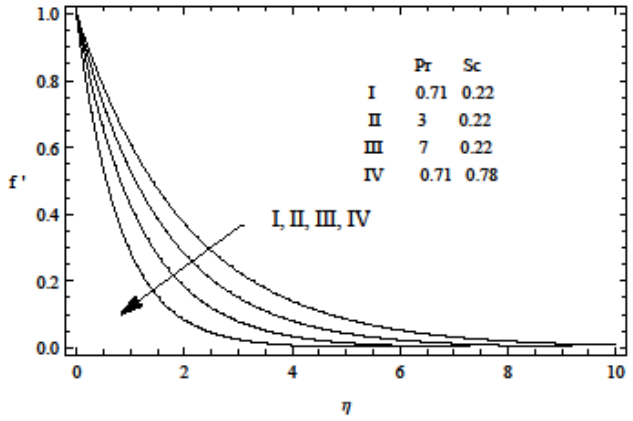

Figure 3: Velocity Profiles against Pr and Sc

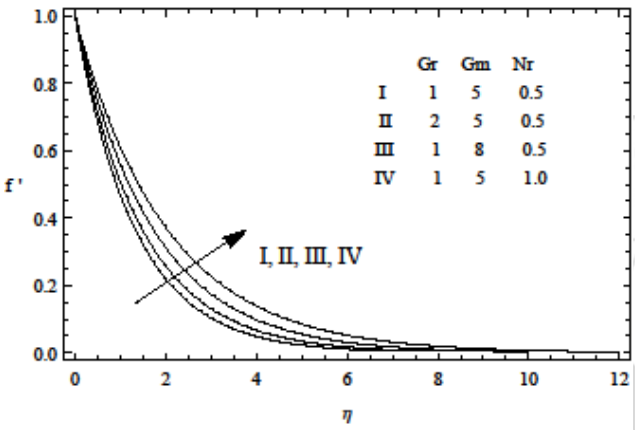

Figure 4: Velocity Profiles against Gr, Gm and Nr

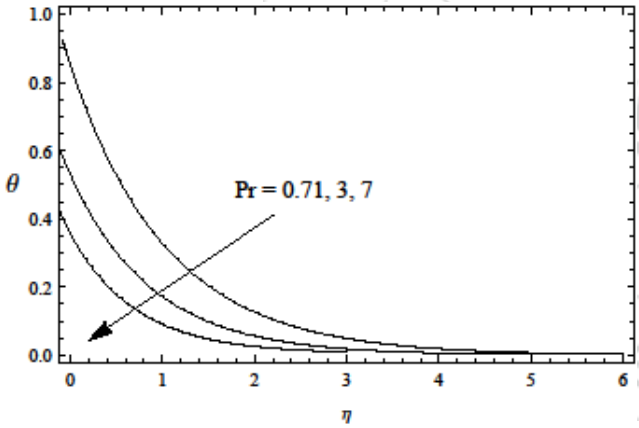

Figure 5: Temperature Profiles against Pr

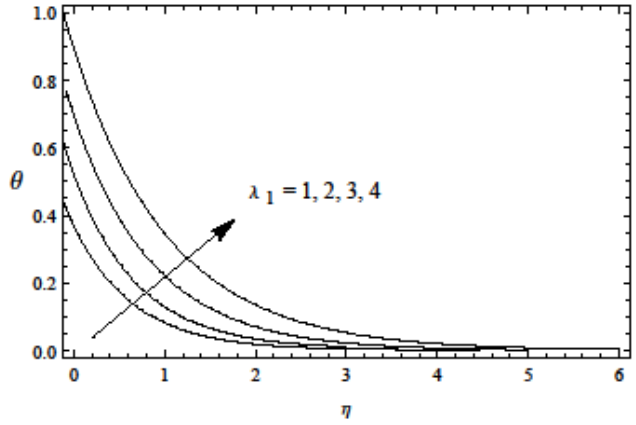

Figure 6: Temperature Profiles against λ1

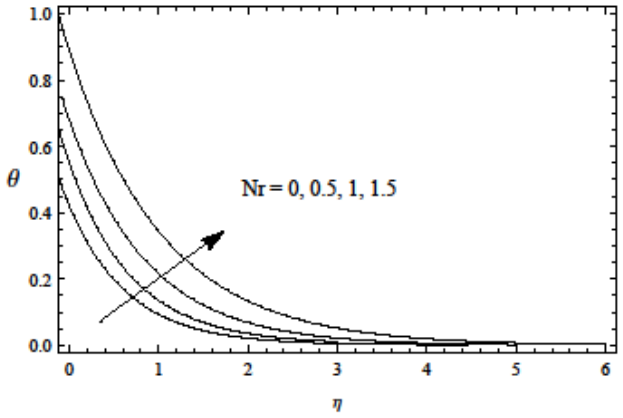

Figure 7: Temperature Profiles against Nr

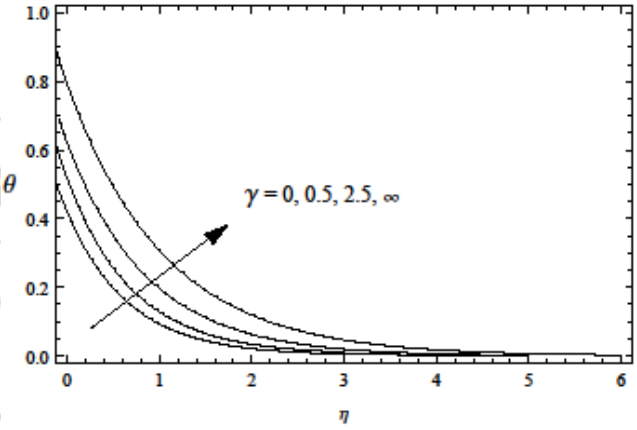

Figure 8: Temperature Profiles against γ

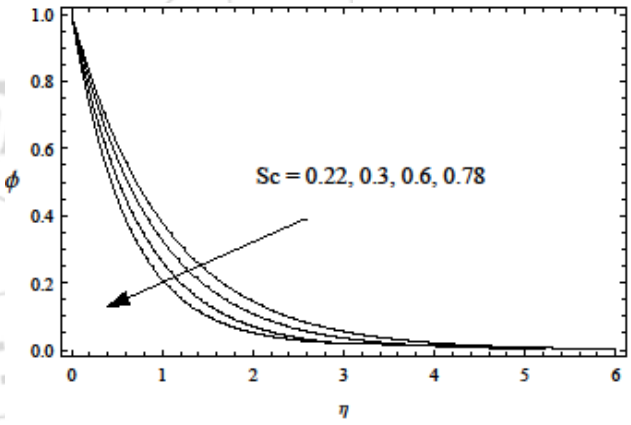

Figure 9: Concentration Profiles against Sc

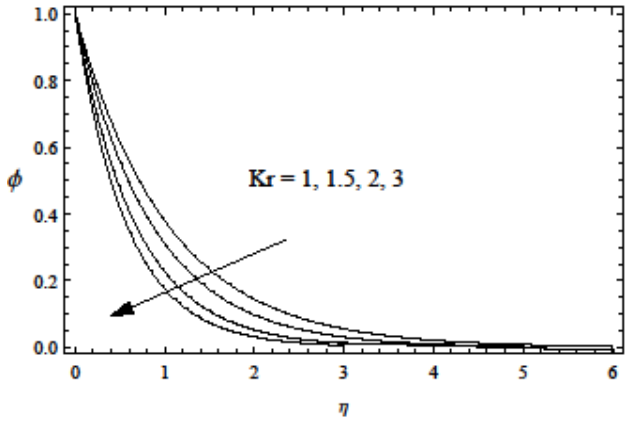

Figure 10: Concentration Profiles against Kr

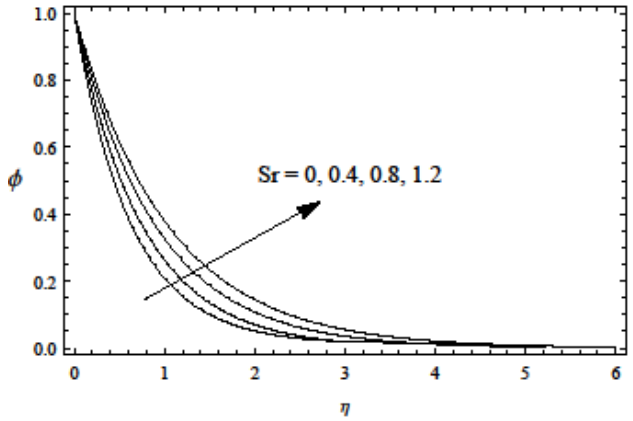

Figure 11: Concentration Profiles against Sr

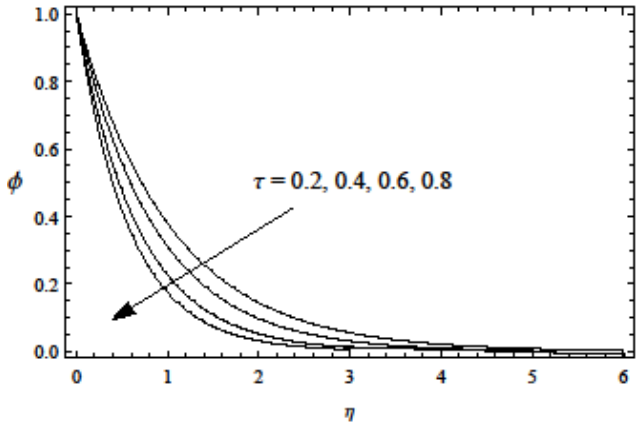

Figure 12: Concentration Profiles against τ

Table 2: Effects of various parameters on stress, Nusselt and Sherwood numbers

M	*Nr*	*γ*	*τ*	λ1	*Kr*	stress	Nusselt number	Sherwood number
2	**0.5**	**0.5**	**0.5**	**1**	**1**	-3.588745	1.058554	1.701452
3	0.5	0.5	0.5	1	1	-3.568885	1.041788	
4	0.5	0.5	0.5	1	1	-3.510088	1.032256	
2	**0.8**	0.5	0.5	1	1	-2.554496	1.144527	
2	**1.0**	0.5	0.5	1	1	-2.112578	1.255478	
2	0.5	**1.0**	0.5	1	1	-4.588456	1.322562	
2	0.5	**1.5**	0.5	1	1	-5.188778	1.855479	
2	0.5	0.5	**1.0**	1	1	-6.878545		1.801452
2	0.5	0.5	**1.5**	1	1	-9.785985		1.851452
2	0.5	0.5	0.5	**2**	1	-2.588777	1.038775	1.928556
2	0.5	0.5	0.5	**3**	1	-1.122063	1.014445	2.118554
2	0.5	0.5	0.5	1	**2**	-1.885456		1.858547
2	0.5	0.5	0.5	1	**3**	-1.041789		1.980985

4. Conclusions

The effect of thermal radiation on MHD boundary layer flow of a non-Newtonian fluid past a stretching sheet with convective surface heat flux in the presence of thermophoresis have been studied. The conclusions are made as the following.

1) The fluid velocity in the boundary layer region increases for increasing the values of thermal radiation parameter and surface convection parameter but the effect is reverse for Hartmann number, thermophoretic parameter and second grade fluid parameter.
2) The temperature profile enhances with increase in the thermal radiation parameter, second grade parameter and surface convection parameter.
3) The chemical species concentration decreases in presence of thermophoresis. Consequently, the rate of mass transfer increases as thermophoretic parameter
4) The skin friction coefficient (in magnitude) decreases with increase of thermal radiation parameter, second grade parameter and surface convection parameter but effect is reverse for thermophoretic parameter.
5) The rate of heat transfer increases for increasing the values of the surface convection parameter and thermal radiation parameter while it decreases with increase in the values of second grade parameter.

References

[1] Abolbashari, M. H., N. Freidoonimehr, F. Nazari and M. M. Rashidi (2015). Analytical modeling of entropy generation for Casson nano-fluid flow induced by a stretching surface. Advanced Powder Technology
[2] Andersson, H. I. and B. S. Dandapat. (1992). Flow of a power law fluid over a stretching sheet, Appl. Anal Continuous Media 1, 339–347.
[3] Bird, R. B., W. E. Stewart and E. N. Lightfoot (1960). Transport Phenomena, Wiley, New York 94–95, 104–105.
[4] Boyd, J., J. M. Buick and S. Green. (2007). Analysis of the Casson and CarreauYasuda non-Newtonian blood models in steady and oscillatory flow using the lattice Boltzmann method. Phys. Fluids 19, 93–103.
[5] Casson, N. and C. C. Mills (1959). Rheology of Disperse Systems, Pergamon, New York, Ch. 5.
[6] Chamkha, A. J., A. M. Aly and M. A. Mansour (2010). Similarity solution for unsteady heat and mass transfer from a stretching surface embedded in a porous medium with suction/injection and chemical reaction effects. Chem. Eng. Commun. 197, 846–858.
[7] Chevalley, J. (1991). An adaptation of the Casson equation for the rheology of chocolate, J. Texture Stud. 22, 219–229.
[8] Churchill, S. W. (1988). Viscous Flows: The Practical Use of Theory, Butterworths, Boston, Ch. 5.
[9] Cokelet, G. R. (1963). The rheology of human blood—measurement near and at zero shear rate Trans. Soc. Rheol 7, 303–317.
[10] Elbashbeshy, E. M. A. and M. A. A. Bazid (2004). Heat transfer over an unsteady stretching surface. Heat Mass Transfer 41, 1-4.

[11] Eldabe, N. T. M. and M. G. E. Salwa (1995). Heat transfer of MHD non-Newtonian Casson fluid flow between two rotating cylinder, J. Phys. Soc. Jpn. 64, 41–64.
[12] Garcia-Ochoa, F. and J. A. Casas. (1994). Apparent yield stress in xanthan gum solutions at low concentrations. Chem. Eng. J. 53, B41–B46.
[13] Hassanien, I. A. (1996). Flow and heat transfer on a continuous flat surface moving in a parallel free stream of power-law fluid. Appl. Model 20, 779–784.
[14] Ishak, A., R. Nazar and I. Pop. (2009). Heat transfer over an unsteady stretching permeable surface with prescribed wall temperature Nonlinear Anal. Real World Appl. 10, 2909–2913.
[15] Joye, D. D. (1998). in: Hazardous and Industrial Wastes, Proc. 30th Mid-Atlantic Industrial Waste Conf., Technomic Publ. Corp., Lancaster, PA/Basel 567–575.
[16] Keimanesha, M., M. M. Rashidi, A. J. Chamkha and R. Jafari (2011). Study of a Third grade non-Newtonian fluid flow between two parallel plates using the multi-step differential transform method. Computers and Mathematics with Applications 62, 2871–2891.
[17] Kirsanov, E. A. and S. V. Remizov. (1999). Application of the Casson model to thixotropic waxy crude oil. Rheol. Acta 38, 172–176.
[18] Kumari, S. V. H. N. K., M. V. R. Murthy, M. C. K. Reddy and Y. V. K. R. Kumar. (2011). Peristaltic pumping of a magnetohydrodynamic Casson fluid in an inclined channel. Adv. Appl. Sci. Res. 2 (2), 428–436.
[19] Mernone, A. V. and J. N. Mazumdar (2002). A mathematical study of peristaltic transport of a Casson fluid. Math. Comp. Mod. 35, 895–912.
[20] Nadeem, S., R. U. Haq and C. Lee. (2012). MHD flow of a Casson fluid over an exponentially shrinking sheet. Scientia Iranica 19, 1550– 1553.
[21] Porwal, P. and V. H. Badshah. (2012). Analysis of steady blood flow with Casson fluid along an inclined plane influenced by the gravity force. Int. J. Theor. Appl. Sci. 4(2), 76–81.
[22] Rashidi, M. M., M. T. RasteGari, M. Asadi and O. Anwar Beg (2012). A Study of non-Newtonian flow and heat transfer over a non-isothermal wedge using the homotopy analysis method. Chem. Eng. Comm. 199, 251-256.
[23] Reher, E. O., D. Haroske and K. Kohler. (1969). Chem. Technol. 21(3), 137– 143.
[24] Sadeghy, K. and M. Sharifi (2004). Local similarity solution for the flow of a 'second-grade' viscoelastic fluid above a moving plate. Int. J. Nonlinear Mech. 39, 1265–1273.
[25] Sajid, M., I. Ahmad, T. Hayat and M. Ayub (2009). Unsteady flow and heat transfer of a second grade fluid over a stretching sheet. Commun. Nonlinear Sci. Num. Simul. 14, 96–108.
[26] Sajid, M., T. Hayat and S. Asgharm. (2007). Nonsimilar analytic solution for MHD flow and heat transfer in a third-order fluid over a stretching sheet. Int. J. Heat Mass Transfer 50, 1723–1736.
[27] Serdar, B. and M. Salih Dokuz. (2006). Threedimensional stagnation point flow of a second grade fluid towards a moving plate. Int. J. Eng. Sci. 44, 49–58.
[28] Sharidan, S., T. Mahmood and I. Pop. (2006). Similarity solutions for the unsteady boundary layer flow and heat transfer due to a stretching sheet. Int. J. Appl. Mech. Eng. 11, 647–54.
[29] Sreenadh, S., A. R. Pallavi and B. h. Satyanarayana. (2011). Flow of a Casson fluid through an inclined tube of non-uniform cross section with multiple stenoses. Adv. Appl. Sci. Res. 2(5), 340–349.
[30] Swati Mukhopadhyay, De Prativa Ranjan, Krishnendu Bhattacharyya and G. C. Layek. (2013). Casson fluid flow over an unsteady stretching surface. Ain Shams Eng. J. 4, 933- 938.
[31] Tsai, R., K. H. Huang and J. S. Huang (2008). Flow and heat transfer over unsteady stretching surface with a non-uniform heat source. Commun. Heat Mass Transfer 35, 1340–1343.
[32] Yih, K. A. (1998). Uniform suction/blowing effect on forced convection about a wedge: uniform heat flux. Acta Mech. 128, 173–181.